An Interference Cancellation Scheme for TFI-OFDM in Time-Variant Large Delay Spread Channel

Yuta IDA[1], *Chang-Jun AHN, Takeshi KAMIO, Hisato FUJISAKA, Kazuhisa HAEIWA*

Faculty of Information Sciences, Hiroshima City Univ., 3-4-1 Ozuka-higashi, Asaminami-ku, Hiroshima, 731-3194 Japan

tyappi@imc.im.hiroshima-cu.ac.jp[1]

Abstract. *In the mobile radio environment, signals are usually impaired by fading and multipath delay phenomenon. In such channels, severe fading of the signal amplitude and inter-symbol-interference (ISI) due to the frequency selectivity of the channel cause an unacceptable degradation of error performance. Orthogonal frequency division multiplexing (OFDM) is an efficient scheme to mitigate the effect of multipath channel. Since it eliminates ISI by inserting guard interval (GI) longer than the delay spread of the channel. In general, the GI is usually designed to be longer than the delay spread of the channel, and is decided after channel measurements in the desired implementation scenario. However, the maximum delay spread is longer than GI, the system performance is significantly degraded. The conventional time-frequency interferometry (TFI) for OFDM does not consider time-variant channel with large delay spread. In this paper, we focus on the large delay spread channel and propose the ISI and inter-carrier-interference (ICI) compensation method for TFI-OFDM.*

Keywords

OFDM, inter-symbol-interference, inter-carrier-interference, guard interval.

1. Introduction

Mobile radio communication systems are increasingly demanded to provide a variety of high-quality multimedia services to mobile users. To meet this demand, modern mobile radio transceiver system must be able to support high capacity, variable bit rate information transmission and high bandwidth efficiency. In the mobile radio environment, signals are usually impaired by fading and multipath delay phenomenon. In such channels, severe fading of the signal amplitude and inter-symbol-interference (ISI) due to the frequency selectivity of the channel cause an unacceptable degradation of error performance. Orthogonal frequency division multiplexing (OFDM) is an efficient scheme to mitigate the effect of multipath channel. Since it eliminates ISI by inserting guard interval (GI) longer than the delay spread of the channel [1], [2]. Therefore, OFDM is generally known as an effective technique for high data rate services. Moreover, OFDM has been chosen for several broadband WLAN standards like IEEE802.11a, IEEE802.11g, and European HIPERLAN/2, and terrestrial digital audio broadcasting (DAB) and digital video broadcasting (DVB) was also proposed for broadband wireless multiple access systems such as IEEE802.16 wireless MAN standard and interactive DVB-T [3], [4].

In OFDM systems, the pilot signal averaging channel estimation is generally used to identify the channel state information (CSI) [5]. In this case, large pilot symbols are required to obtain an accurate CSI. As a result, the total transmission rate is degraded due to transmission of large pilot symbols. Recently, carrier interferometry (CI) has been proposed to identify the CSI of multiple-input multiple-output (MIMO). However, the CI used only one phase shifted pilot signal to distinguish all the CSI for the combination of transmitter and receiver antenna elements. In this case, without noise whitening, each detected channel impulse response is affected by noise [6]. Therefore, the pilot signal averaging process is necessary for improving the accuracy of CSI [7]. To reduce this problem, time-frequency interferometry (TFI) for OFDM has been proposed [8] – [10].

In general, the GI is usually designed to be longer than the delay spread of the channel, and is decided after channel measurements in the desired implementation scenario. However, if the maximum delay spread is longer than GI, the system performance is significantly degraded. TFI-OFDM does not consider time-variant channel with large delay spread. In this paper, we focus on the large delay spread channel and evaluate the performance of the TFI-OFDM. Until this time, several schemes have been proposed to mitigate the ISI due to the large delay spread channel. Gejoh proposed ISI reduction method by increasing the GI to overcome the above problems [11]. However, transmission efficiency is deteriorated, and transmit power is increased. Lee proposed double window cancellation and combining as ISI canceller scheme [12]. However the complexity is a serious problem. Suyama proposed several frequency domain ISI cancellering schemes such as a smoothed FFT windows and decision feedback equalizer (DFE) [13]. However it is very sensitive to the severe frequency selective channel, and also it has a power loss by

removing GI. To reduce above-mentioned problems, in this paper, we propose a novel time domain ISI cancellation scheme with replica signal based inter-carrier-interference (ICI) compensation for TFI-OFDM [14]. This paper is organized as follows. Configuration of the proposed system is described in Section 2. In Section 3, we show the computer simulation results. Finally, the conclusion is given in Section 4.

2. Proposed System

This section describes the proposed system, which employs time division multiplexing (TDM) transmission for multiple users. The proposed system is illustrated in Fig. 2.

2.1 Channel Model

We assume that a propagation channel consists of L discrete paths with different time delays. The impulse response $h(\tau,t)$ is represented as

$$h(\tau,t)=\sum_{l=0}^{L-1}h_l(t)\delta(\tau-\tau_l) \tag{1}$$

where h_l and τ_l are complex channel gain and the time delay of lth propagation path, respectively, and $\sum_{l=0}^{L-1}E\left|h_l^2\right|=1$, where $E|\cdot|$ denotes the ensemble average operation. The channel transfer function $H(f,t)$ is the Fourier transform of $h(\tau,t)$ and is given by

$$\begin{aligned}H(f,t)&=\int_0^{\infty}h(\tau,t)\exp(-j2\pi f\tau)d\tau\\&=\sum_{l=0}^{L-1}h_l(t)\exp(-j2\pi f\tau_l).\end{aligned} \tag{2}$$

2.2 CI/OFDM

The OFDM system transmit signal can be expressed in its equivalent baseband representation as

$$\begin{aligned}s_{ci}(t)=\sum_{i=0}^{N_p+N_d-1}g(t-iT)\cdot\left\{\sqrt{\frac{2S}{N_c}}\sum_{k=0}^{N_c-1}d(k,i)\right.\\\left.\cdot\exp[j2\pi(t-iT)k/T_s]\right\}\end{aligned} \tag{3}$$

where N_d and N_p are the number of data and pilot symbols, N_c is the number of carriers, T_s is the effective symbol length, S is the average transmitting power, T is the OFDM symbol length, respectively. The guard interval T_g is inserted in order to eliminate the ISI due to the multi-path fading, and hence, we have

$$T=T_s+T_g. \tag{4}$$

In OFDM systems, T_g is generally considered as $T_s/4$ or $T_s/5$. Thus, we assume $T_g = T_s/4$ in this paper. In (3), $g(t)$ is the transmission pulse given by

$$g(t)=\begin{cases}1 & \text{for } -T_g\le t\le T_s,\\0 & \text{otherwise}.\end{cases} \tag{5}$$

The conceptual figure of CI/OFDM is shown in Fig. 1. For $0 \le i \le N_p - 1$, the transmitted pilot signal of the kth subcarrier in CI/OFDM is given by

$$d(k,i)=\exp(-j2\pi kT_{os}/T_s) \tag{6}$$

where T_{os} is the phase offset in the frequency domain. In this case, the CI/OFDM signal obtains T_{os} time shifted impulse signal as shown in Fig. 1(b). By applying this concept to MIMO systems, we can multiplex the impulse responses without overlapping to each other on the time domain, and can identify the CSI. However, the CI used only one phase shifted pilot signal to distinguish all the CSI for the combination of transmitter and receiver antenna elements. In this case, without noise whitening, each detected channel impulse response is affected by noise [6]. Therefore, the pilot signal averaging process is necessary for improving the accuracy of CSI [7]. To reduce this problem, TFI-OFDM has been proposed.

2.3 TFI-OFDM

The transmitter block diagram of proposed system is shown in Fig. 2(a). Firstly, the coded binary data is modulated, and N_p pilot symbols are appended at the beginning of the sequence. The TFI-OFDM system transmit signal can be expressed in its equivalent baseband representation as

$$\begin{aligned}s(t)=\sum_{i=0}^{N_p+N_d-1}g(t-iT)\cdot\left\{\sqrt{\frac{2S}{N_c}}\sum_{k=0}^{N_c-1}u(k,i)\right.\\\left.\cdot\exp[j2\pi(t-iT)k/T_s]\right\}.\end{aligned} \tag{7}$$

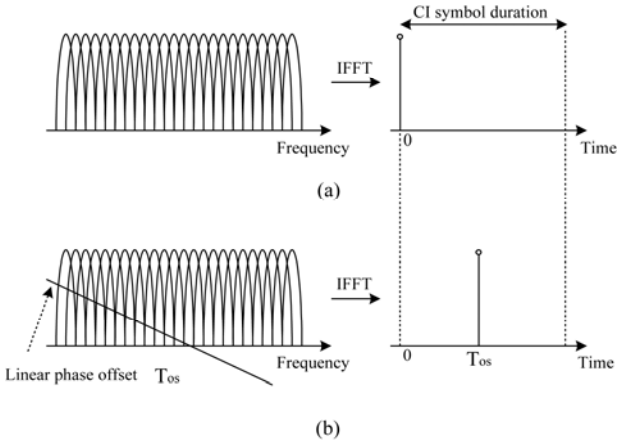

Fig. 1. The concept of carrier interferometry.

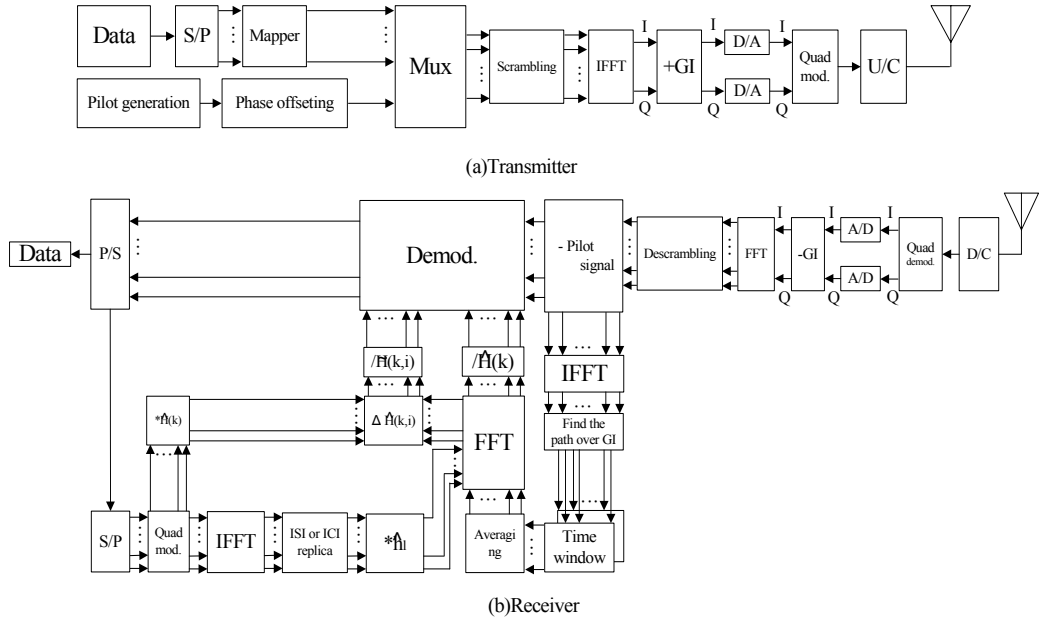

Fig. 2. Proposed system.

The frequency separation between adjacent orthogonal subcarriers is $1/T_s$ and can be expressed, by using the kth subcarrier of the ith modulated symbol $d(k,i)$ with $|d(k,i)| = 1$ for $N_p \le i \le N_p + N_d - 1$, as

$$u(k,i) = c_{PN}(k) \cdot d(k,i) \tag{8}$$

where c_{PN} is a long pseudo-noise (PN) sequence as a scrambling code to reduce the peak average power ratio (PAPR). For example, if we consider "1" chip, the phase rotation of the signal is 0 deg. Meanwhile, if we consider "–1" chip, the phase rotation of the signal is 180 deg. Therefore, we can reduce the PAPR with considering the randomized phase of the signal. In this case, the chip rate c_{PN} is the same as the sampling rate of the OFDM signal. For $0 \le i \le N_p - 1$, the transmitted pilot signal of the kth subcarrier is given by

$$d(k,i) = \exp(-j2\pi k/T_s) + \exp(-j4\pi k T_g/T_s). \tag{9}$$

After IFFT operation, (9) shows two time impulses as shown in Fig. 3(a). This pilot signal pattern is the originality of TFI-OFDM. Moreover, due to the superposition of (9), the transmit power of pilot signals is 1/2 for $0 \le i \le N_p - 1$. For example, owing to (9), we obtain $\sum_{k=0}^{N_c-1} d(k,i) = \{1,0,\cdots 1,0\}$ as the pilot signals. In this case, since pilot signal includes "0" component, we can identify the CSI with the half of transmit power of pilot signals compared with the conventional pilot based system.

The receiver structure is illustrated in Fig. 2(b). By applying the FFT operation, the received signal $r(t)$ is resolved into N_c subcarriers. The received signal $r(t)$ in the equivalent baseband representation can be expressed as

$$r(t) = \int_{-\infty}^{\infty} h(\tau,t)s(t-\tau)d\tau + n(t) \tag{10}$$

where $n(t)$ is additive white Gaussian noise (AWGN) with a single sided power spectral density of N_0. The kth subcarrier $\tilde{r}(k,i)$ is given by

$$\begin{aligned}\tilde{r}(k,i) &= \frac{1}{T_s}\int_{iT}^{iT+T_s} r(t)\exp[-j2\pi(t-iT)k/T_s]dt \\ &= \sqrt{\frac{2S}{N_c}}\sum_{e=0}^{N_c-1} u(e,i)\cdot\frac{1}{T_s}\int_0^{T_s}\exp[j2\pi \\ &\quad\cdot(e-k)t/T_s]\cdot\left\{\int_{-\infty}^{\infty} h(\tau,t+iT)g(t-\tau)\right. \\ &\quad\left.\cdot\exp(-j2\pi e\tau/T_s)d\tau\right\}dt + \hat{n}(k,i)\end{aligned} \tag{11}$$

where $\hat{n}(k,i)$ is AWGN noise with zero-mean and a variance of $2N_0/T_s$. After abbreviating, (11) can be rewritten as

$$\begin{aligned}\tilde{r}(k,i) &\approx \frac{1}{T_s}\sqrt{\frac{2S}{N_c}}\sum_{e=0}^{N_c-1} u(e,i)\cdot\int_0^{T_s}\exp[j2\pi \\ &\quad\cdot(e-k)t/T_s]\cdot\left\{\int_{-\infty}^{\infty} h(\tau,t+iT)\right. \\ &\quad\left.\cdot g(t-\tau)\exp(-j2\pi e\tau/T_s)d\tau\right\}dt + \hat{n}(k,i) \\ &= \sqrt{\frac{2S}{N_c}}H(k,i)u(k,i) + \hat{n}(k,i).\end{aligned} \tag{12}$$

After descrambling, the output signal $r(k,i)$ is given by

$$\begin{aligned}r(k,i) &= \frac{c_{PN}^*(k)}{|c_{PN}(k)|^2}\{\tilde{r}(k,i)\} \\ &= \sqrt{\frac{2S}{N_c}}H(k,i)d(k,i) + \hat{n}(k,i)\end{aligned} \tag{13}$$

where $c^*_{PN}(k)/|c_{PN}(k)|^2$ is the descrambling operation. Observing (12) and (13), the noise components are the same notation. In this paper, descrambling operation is to rotate the phase of each subcarrier by using PN codes. In this case, the noise components of (12) and (13) are the same notation. From this reason, we used the same notation $\hat{n}(k,i)$ as a noise variance of (12) and (13). Since $T_g = T_s/4$, TFI-OFDM can multiplex the same impulse responses in twice on the time domain as shown in Fig. 3(b). After the pilot signal separation, the pilot signal is converted to the time domain signal $\hat{r}(t)$ again as

$$\begin{aligned}\hat{r}(t) &= \sum_{i=0}^{N_p-1}\sqrt{\frac{2P}{N_c}}\sum_{k=0}^{N_c-1} r(k,i)\exp\left[j2\pi(t-iT)k/T_s\right] \\ &= \sum_{i=0}^{N_p-1}\sqrt{\frac{2P}{N_c}}h(\tau,t+iT)\sum_{k=0}^{N_c-1} d(k,i) \\ &\quad\cdot\exp\left[j2\pi(t-iT)k/T_s\right]+\tilde{n}(t) \\ &= \sum_{i=0}^{N_p-1}\sqrt{\frac{2P}{N_c}}\sum_{l=0}^{L-1} h_l(t+iT) \\ &\quad\cdot\frac{1}{\sqrt{2}}\left\{\delta(\tau-\tau_l)+\delta(\tau-\tau_l-2T_g)\right\}+\tilde{n}(t)\end{aligned} \tag{14}$$

where P is the power of pilot signals and $\tilde{n}(t)$ is the noise component. The converted time domain signal $\hat{r}(t)$ is shown in Fig. 3(b). From equation (9), $\sum_{k=0}^{N_c-1} d(k,i)\exp\left[j2\pi(t-iT)k/T_s\right]$ shows two impulses

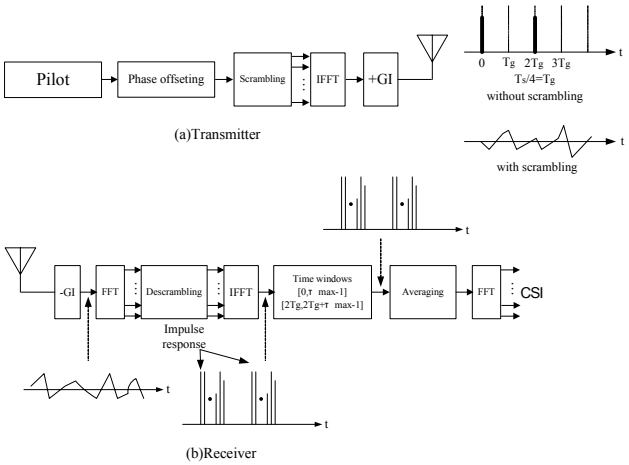

Fig. 3. The concept of TFI-OFDM system.

with time shift as $\delta(\tau - 2T_g)$, and the output signals are equivalent to time domain multiplexed impulse responses. By averaging of these impulse responses within two time windows as $[0, T_g]$, $[2T_g, 3T_g]$, we can reduce the noise effect. Moreover, we assign the null signals on the spectrum $[T_g, 2T_g]$, $[3T_g, 4T_g]$. Therefore, the estimated impulse response of the kth pilot subcarrier $\hat{H}(k)$ is obtained by

$$\begin{aligned}\hat{H}(k) &= \frac{1}{\sqrt{P/N_c}}\sum_{e=0}^{N_c-1}\frac{1}{T_s}\int_0^{T_s}\left\{\sum_{l=0}^{L-1} h_l(t+iT)\right. \\ &\quad\cdot\int_{-\infty}^{\infty}\left\{\delta(\tau-\tau_l)+\delta(\tau-\tau_l-2T_g)\right\} \\ &\quad\left.\cdot\exp(-j2\pi e\tau/T_s)d\tau\right\}dt+\eta(k)\end{aligned} \tag{15}$$

where $\eta(k)$ is AWGN component with $E\left[|\eta(k)|\right]^2 = E\left[|\hat{n}(k,i)/2|\right]^2 = \sigma^2/2$. Due to null signals assignment on $[T_g, 2T_g]$, $[3T_g, 4T_g]$, the noise variance of $\eta(k)$ is reduced as $\hat{n}(k,i)/2$. For $\tau_L < T_g$, the faded channel is easily compensated by using (15), where τ_L is the maximum delay spread. Alternately, (14) for $N_p \le i \le N_p + N_d - 1$ can be rewritten in matrix form as

$$\mathbf{R_i} = \mathbf{H_i}\,\mathrm{F}\,\mathbf{D_i} + \mathbf{N_i} \tag{16}$$

where $\mathbf{H_i}$ is the $N_c \times N_c$ time-domain matrix for the ith symbol, $\mathbf{N_i}$ is the $N_c \times 1$ noise matrix, F is the IFFT operation, respectively. For $\tau_L > T_g$, (16) can be written as

$$\mathbf{R_i} = \mathbf{H_{i-1,isi}}\,\mathrm{F}\,\mathbf{D_{i-1}} + \mathbf{H_{i,ici}}\,\mathrm{F}\,\mathbf{D_i} + \mathbf{N_i} \tag{17}$$

where $\mathbf{H_{i-1,isi}}$ and $\mathbf{H_{i,ici}}$ denote ISI and ICI channel matrices for the $(i-1)$th and ith symbols.

2.4 Conventional ISI and ICI Equalization

In general, the first symbol of the received signal has no ISI for $\tau_L > T_g$ [12] – [14]. In this case, (17) can be written as

$$\mathbf{R_i} = \mathbf{H_{i,ici}}\,\mathrm{F}\,\mathbf{D_i} + \mathbf{N_i}\,. \tag{18}$$

From (18), the equalization coefficient can be easily calculated by the Hermitian of $\mathbf{H_{i,ici}}$F. However, since the symbols behind the first symbol include the ISI, ISI equalization should be performed with the previously detected symbol $\hat{\mathbf{D}}_{\mathbf{i-1}}$ and ISI channel matrix $\mathbf{H_{i-1,isi}}$. In this case, the ISI equalized signal $\tilde{\mathbf{R}}_{\mathbf{i}}$ is given by

$$\begin{aligned}\tilde{\mathbf{R}}_{\mathbf{i}} &= \mathbf{R_i} - \mathbf{H_{i-1,isi}}\,\mathrm{F}\,\mathbf{D_{i-1}} + \tilde{\mathbf{N}}_{\mathbf{i}} \\ &= \boldsymbol{\lambda}_{\mathbf{i,ici}}\,\mathrm{F}\,\mathbf{D_i} + \tilde{\mathbf{N}}_{\mathbf{i}}\end{aligned} \tag{19}$$

where $\tilde{\mathbf{N}}_{\mathbf{i}}$ is the noise term with the residual ISI, $\boldsymbol{\lambda}_{\mathbf{i,ici}}$ is the remained ICI channel matrix, respectively. Observing (19), since the residual ISI and ICI terms exist, a further equalization processing is necessary. Zero-forcing (ZF) uses a combining weight that is inversely proportional to the estimated channel matrix $\boldsymbol{\lambda}_{\mathbf{i,ici}}$, in order to mitigate the residual ISI and ICI. The ZF weight is given by

$$\boldsymbol{\omega}_{\mathbf{i,ZF}} = \frac{1}{\boldsymbol{\lambda}_{\mathbf{i,ici}}\cdot\mathrm{F}}. \tag{20}$$

By using (20), the detected signal $\hat{\mathbf{D}}_{\mathbf{i}}$ can be written as

$$\begin{aligned}\hat{\mathbf{D}}_{\mathbf{i}} &= \boldsymbol{\omega}_{\mathbf{i,ZF}} \cdot \boldsymbol{\lambda}_{\mathbf{i,ici}} \,\mathrm{F}\, \mathbf{D}_{\mathbf{i}} + \boldsymbol{\omega}_{\mathbf{i,ZF}} \cdot \widetilde{\mathbf{N}}_{\mathbf{i}} \\ &= \mathbf{D}_{\mathbf{i}} + \frac{\widetilde{\mathbf{N}}_{\mathbf{i}}}{\boldsymbol{\lambda}_{\mathbf{i,ici}} \cdot \mathrm{F}}.\end{aligned} \tag{21}$$

From (21), we can observe that the first term is the desired signal, the second term is a noise term. From the second term, ZF scheme can equalize the residual ISI and ICI, but it enhances the noise term due to the residual ISI and ICI. If we eliminate the ICI of (21), the detected signal $\hat{\mathbf{D}}_{\mathbf{i}}$ is accurately detected.

2.5 Replica Signal Insertion Based ICI Equalization

From (19), ISI is subtracted from the received signal. However, the orthogonality is destroyed by the subtracted signal due to the ISI compensation. To avoid the noise enhancement due to the residual ISI and ICI, we consider the orthogonality reconstruction with inserting the subtracted signal due to ISI compensation. The ICI equalized signal $\breve{\mathbf{R}}_{\mathbf{i}}$ with inserting subtracted the part of the signal using the previously detected $\hat{\mathbf{D}}_{\mathbf{i}}$ is given by

$$\begin{aligned}\breve{\mathbf{R}}_{\mathbf{i}} &= \mathbf{R}_{\mathbf{i}} - \mathbf{H}_{\mathbf{i-1,isi}} \,\mathrm{F}\, \mathbf{D}_{\mathbf{i-1}} + \mathbf{H}_{\mathbf{i,ici}} \,\mathrm{F}\, \hat{\mathbf{D}}_{\mathbf{i}} + \breve{\mathbf{N}}_{\mathbf{i}} \\ &= \boldsymbol{\lambda}_{\mathbf{i,pro}} \,\mathrm{F}\, \mathbf{D}_{\mathbf{i}} + \breve{\mathbf{N}}_{\mathbf{i}},\end{aligned} \tag{22}$$

where $\breve{\mathbf{N}}_{\mathbf{i}}$ is the noise term with the residual ISI and the residual ICI, $\boldsymbol{\lambda}_{\mathbf{i,pro}}$ is the ISI and ICI subtracted channel matrix, respectively. By using Eq. (22), the detected signal $\widetilde{\mathbf{D}}_{\mathbf{i}}$ can be written as

$$\begin{aligned}\widetilde{\mathbf{D}}_{\mathbf{i}} &= \widetilde{\boldsymbol{\omega}}_{\mathbf{i,pro}} \cdot \boldsymbol{\lambda}_{\mathbf{i,pro}} \,\mathrm{F}\, \mathbf{D}_{\mathbf{i}} + \widetilde{\boldsymbol{\omega}}_{\mathbf{i,pro}} \cdot \breve{\mathbf{N}}_{\mathbf{i}} \\ &= \mathbf{D}_{\mathbf{i}} + \frac{\breve{\mathbf{N}}_{\mathbf{i}}}{\boldsymbol{\lambda}_{\mathbf{i,pro}} \cdot \mathrm{F}}\end{aligned} \tag{23}$$

where $\widetilde{\boldsymbol{\omega}}_{\mathbf{i,pro}} = 1/\left(\boldsymbol{\lambda}_{\mathbf{i,pro}} \cdot \mathrm{F}\right)$. Observing (21), (23), the proposed method using the orthogonality reconstruction with inserting the subtracted signal due to ISI compensation can reduce the enhancement of the noise term. Therefore, the detected signal $\widetilde{\mathbf{D}}_{\mathbf{i}}$ is accurately detected to compare with $\hat{\mathbf{D}}_{\mathbf{i}}$. However, the detection accuracy is dependent on the channel identification. $\boldsymbol{\lambda}_{\mathbf{i,pro}}$ is calculated by $\mathbf{H}_{\mathbf{i-1,isi}}$ and $\mathbf{H}_{\mathbf{i,ici}}$, thus, the estimation errors are included in the detected signal. To eliminate the estimation errors, we calculate the estimation errors as

$$\Delta\hat{H}(k,i) = \frac{\breve{d}(k,i)}{\widetilde{d}(k,i) \cdot \hat{H}(k)} \tag{24}$$

where $\breve{d}(k,i)$ is the frequency domain components of $\breve{\mathbf{R}}_{\mathbf{i}}$, $\widetilde{d}(k,i)$ is the frequency domain components of $\widetilde{\mathbf{D}}_{\mathbf{i}}$. From (24), the estimation errors include the noise. In order to control the influence of noise, we average the previous symbols. As a result, the averaged estimation errors $\varepsilon(k,i)$ is given by

$$\varepsilon(k,i) = \frac{\Delta\hat{H}(k,i) + \Delta\hat{H}(k,i-1)}{2}. \tag{25}$$

Therefore, the improved CSI is given by

$$\widetilde{H}(k,i) = \hat{H}(k) \cdot \varepsilon(k,i). \tag{26}$$

By using $\widetilde{H}(k,i)$, we compensate the channel estimation error. The detected data signal $\bar{d}(k,i)$ is given by

$$\bar{d}(k,i) = \frac{\breve{d}(k,i)}{\widetilde{H}(k,i)}. \tag{27}$$

3. Computer Simulation Results

In this section, we show the performance of the proposed method. Fig. 2 shows a simulation model of the proposed system. On the transmitter, the pilot signals are assigned for each transmitter using (9). In this case, the proposed system can multiplex the same impulse responses in the receiver antenna in twice on the time domain without overlapping to each other as shown in Fig. 3(a). The coded bits are QPSK modulated, and then the pilot signal and data signal are multiplexed with scrambling using PN code to reduce the PAPR. The OFDM time signals are generated by an IFFT and transmitted to frequency selective and time variant radio channel after cyclic extensions have been inserted. The transmitted signals are subject to broadband channel propagation. In the simulation, we assume that OFDM symbol period is 5 μs, guard interval is 1 μs, and channel model is L = 2 paths Rayleigh fadings. The maximum Doppler frequencies are assumed to be 10, 300, and 600 Hz. In the receiver, the guard interval is erased from the received signals and S/P converted. The parallel sequences are passed to an FFT operator, which converts the signal back to the frequency domain. After descrambling and IFFT, each impulse response can be estimated by extracting and averaging twice impulse responses using the time windows with (15) as shown in Fig. 3(b). After FFT operation, the frequency domain data signal is demodulated using the estimated channel impulse response. Since the detected data signals include the ISI and ICI, it is necessary to remove them. ISI equalization should be performed with the previous detected symbol and ISI channel matrix as (19). By using ZF, the ISI and ICI can be equalized, but it enhances the noise term for a deep faded subcarrier. To overcome this problem, replica signal insertion based ICI equalization is considered. From (19), ISI is deducted from the received signal. However, the orthogonality is destroyed by the deducted signal due to the ISI compensation. By using the replica signal insertion, ICI is deducted as (23). From (23), the estimation errors are included in the detected signal. To eliminate the estimation errors, the proposed method calculates the estimation errors as (25)

and (26). Finally, by using (26), the data signal is detected. As Fig. 4, the packet consists of $N_p = 1$ pilot symbol and $N_d = 20$ data symbols. The pilot signal is assigned on the frequency domain with "1" and "0" alternately. Tab. 1 shows the simulation parameters.

Data modulation	QPSK
Data detection	Coherent
Symbol duration	5 μs
Frame size	21 symbols ($N_p = 1$, $N_d = 20$)
FFT size	64
Number of carriers	64
Guard interval	16 sample times
Fading	2 path Rayleigh fading
Doppler frequency	10, 300, 600 Hz

Tab. 1. Simulation parameters.

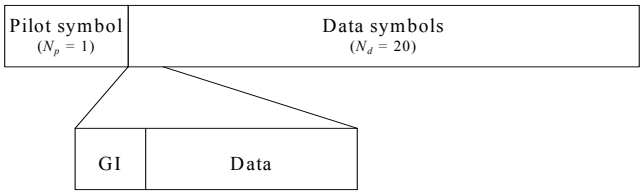

Fig. 4. The packet structure in the simulation.

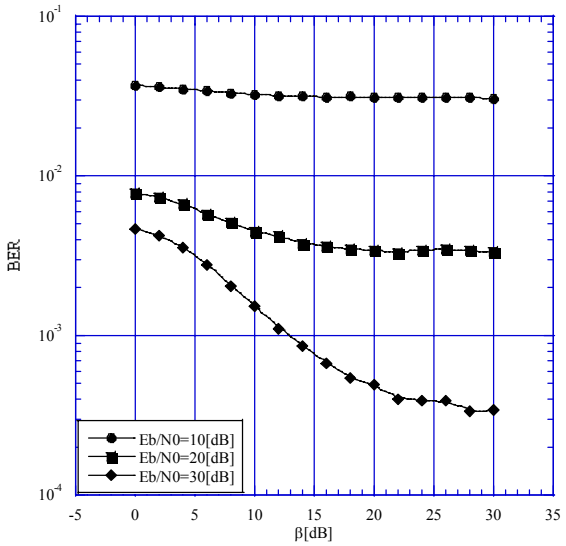

Fig. 5. BER versus the total power ratio β for E_b/N_0 = 10, 20, and 30 dBs and Doppler frequency of 10 Hz.

Fig. 5 shows the BER versus the total power ratio β for E_b/N_0 = 10, 20, and 30 dBs and Doppler frequency of 10 Hz. In order to compare the performance of different total power ratio between inside and outside of GI, the electric power ratio β is defined as

$$\beta = 10\log_{10}\left|\frac{P_{in\_GI}}{P_{out\_GI}}\right| \tag{28}$$

where P_{in_GI} and P_{out_GI} are the total power of paths of inside and outside as GI. From the simulation results, the BER performances are saturated when $\beta \geq 22$. It means that ISI and ICI are not serious for the system performance. Therefore, we can abbreviate the compensation processing for ISI and ICI.

Fig. 6 shows the BER of the proposed method and the conventional methods for β = 0 and Doppler frequency of 10 Hz. For a delay spread that is longer than the GI, the BER rises rapidly due to ISI and ICI. From the simulation results, the BER with a delay spread that is longer than GI, show about 10 times compared with no ISI and ICI case. In the ISI compensation with ZF as a ICI compensation method, the BER performance shows the error floor. This is because the ICI is still remained and the ICI and noise components are amplified by ZF. The proposed method shows the approximately same BER performance like the case with no ISI and ICI. This is because the proposed method can mitigate the ISI and ICI by using the accurate CSI that estimated from the replica signal and the received signal.

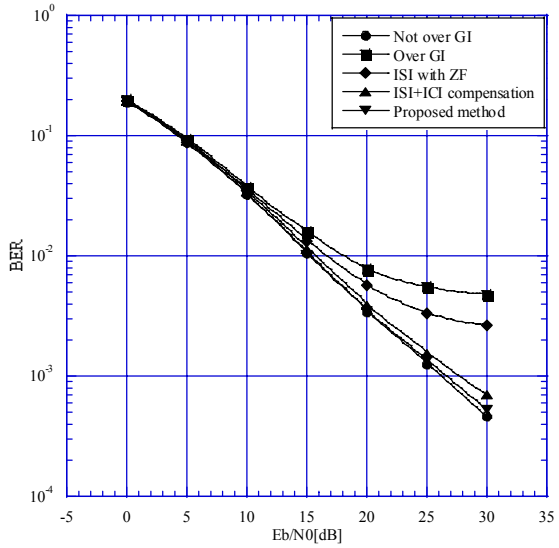

Fig. 6. BER of not over the GI, over the GI, the ISI with ZF, the ISI+ICI compensation, and the proposed method for β = 0 dB and Doppler frequency of 10 Hz.

Figs. 7 and 8 show the BER of the proposed method and the conventional methods for β = 10 and 20 and Doppler frequency of 10 Hz. For β = 10, the BER with a delay spread that is longer than GI, shows about 3 times compared with no ISI and ICI case. The proposed method and the conventional ISI+ICI method show the amount of the interference is degraded by increasing β. Therefore, the estimation error is also degraded. For β = 20, the BER with a delay spread that is longer than GI, shows approximately same BER performance. This is because the approximately same performance compared with no ISI and ICI case. As a result, we can adaptively abbreviate the compensation complexity with considering β.

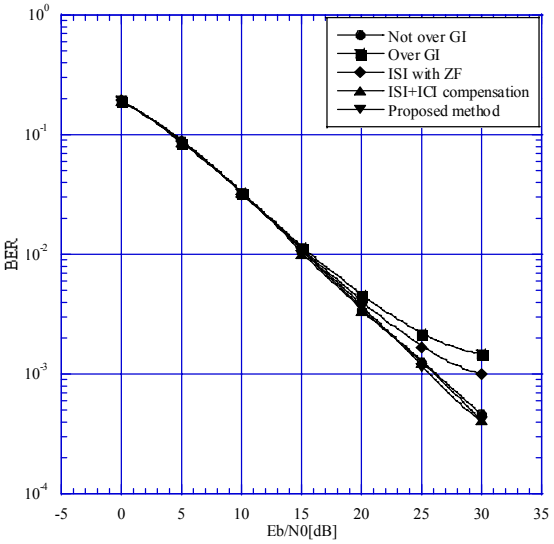

Fig. 7. BER of not over the GI, over the GI, the ISI with ZF, the ISI+ICI compensation, and the proposed method for β = 10 dB and Doppler frequency of 10 Hz.

Fig. 9 shows the BER of not over the GI, over the GI, and the proposed method for β = 0 and Doppler frequencies of 10, 300, and 600 Hz. From the simulation results, the proposed method shows 1 dB penalty compared with no ISI and ICI case for Doppler frequency of 10 Hz. On the other hands, the proposed method and no ISI and ICI case show the approximately same BER performance for Doppler frequencies of 300 and 600 Hz. This is because the influence of high Doppler frequency is larger than it of a delay spread that is longer than GI. Therefore, the proposed method maintains an interference cancelling property in high Doppler frequency.

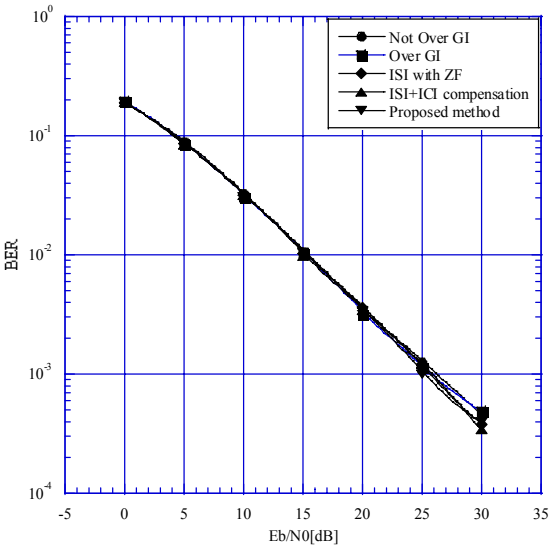

Fig. 8. BER of not over the GI, over the GI, the ISI with ZF, the ISI+ICI compensation, and the proposed method for β = 20 dB and Doppler frequency of 10 Hz.

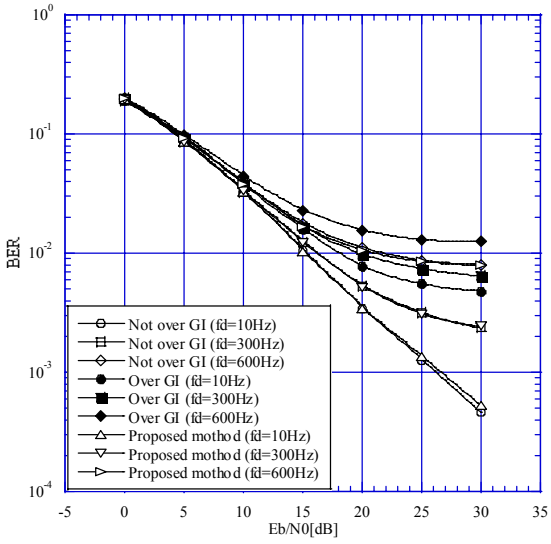

Fig. 9 BER of not over the GI, over the GI, and the proposed method for β = 0 dB and Doppler frequencies of 10, 300, and 600 Hz.

4. Conclusion

In this paper, we focus on the large delay spread channel and propose the ISI and ICI compensation method for TFI-OFDM. From the simulation results, it is shown that the proposed method achieves the approximately same BER performance like the case with no ISI and ICI. For $\beta > 22$, the BER performances are saturated. Moreover, the proposed method and the conventional ISI+ICI method show the approximately same BER performance by increasing β. Consequently, we can adaptively abbreviate the compensation complexity with considering β. For Doppler frequencies of 300 and 600 Hz, the proposed method and not over the GI show the approximately same BER performance. Therefore, the proposed method can also apply high Doppler frequency case.

References

[1] CIMINI, L. Analysis and simulation of digital mobile channel using OFDM. *IEEE Trans. Commun.*, 1985, vol. 33, no. 7, pp. 665 to 675.

[2] BINGHAM, J.A.C. Multicarrier modulation for data transmission: An idea whose time has come. *IEEE Commun. Mag.*, May 1990, vol. 28, pp. 5-14.

[3] ETSI ETS 301 958, *Digital Video Broadcasting (DVB): Interaction Channel for Digital Terrestrial Television (RCT) Incorporating Multiple Access OFDM*. ETSI, Tech.Rep., March 2002.

[4] KOFFMAN, I., ROMAN, V. Broadband wireless access solutions based on OFDM access in IEEE802.16. *IEEE Commun. Mag.*, April 2002, vol. 40, pp. 96-103.

[5] AHN, C., SASASE, I. The effects of modulation combination, target BER, Doppler frequency, and adaptive interval on the performance of adaptive OFDM in broadband mobile channel. *IEEE Trans. Consum. Electron*., Feb. 1999, vol. 48, no. 1, pp.167 to 174.

[6] YOKOMAKURA, K., SAMPEI, S., MORINAGA, N. A carrier interferometry based channel estimation technique for one-cell reuse MIMO-OFDM/TDMA cellular systems. In *Proc. VTC 2006*, pp. 1733-1737, 2006.

[7] YOKOMAKURA, K., SAMPEI, S., HARADA, H., MORINAGA, N. A channel estimation technique for dynamic parameter controlled-OF/TDMA systems. In *Proc. IEEE PIMRC*, vol.1, pp. 644 to 648, 2005.

[8] AHN, C. Accurate channel identification with time-frequency interferometry for OFDM. *IEICE Trans. Fundamentals*, vol. E90-A, no. 11, pp. 2641-2645, Nov. 2007.

[9] YOFUNE, M., AHN, C., KAMIO, T., FUJISAKA, H., HAEIWA, K. Decision direct and linear prediction based fast fading compensation for TFI-OFDM. In *Proc. of ITC-CSCC2008*, pp. 81 to 84, July 2008.

[10] YOSHIMURA, T., AHN, C., KAMIO, T., FUJISAKA, H., HAEIWA, K. Performance enhancement of TFI-OFDM with path selection based channel identification, In *Proc. of ITC-CSCC2008*, pp. 1313-1316, July 2008.

[11] GEJOH, N., KARASAWA, Y. OFDM transmission characteristics in multipath environment where the delay spreading exceeds the guard interval analyzed based on the ETP model. *IEICE Trans. Commun.*, Nov. 2002, vol.J 85-B, no. 11, pp. 1904-1912.

[12] LEE, J. H., KISHIYAMA, Y., OHTSUKI, T., NAKAGAWA, M. Double window cancellation and combining for OFDM in time-invariant large delay spread channel. *IEICE Trans. Fundamentals,* vol. E90-A, no. 10, pp. 2066-2078, Oct. 2007.

[13] SUYAMA, S., ITO, M., SUZUKI, H., FUKAWA, K. A scattered pilot OFDM receiver with equalization for multipath environments with delay difference greater than guard interval. *IEICE Trans. Communications*, vol. E86-B, no. 1, pp. 275-282, Jan. 2003.

[14] IDA, Y., AHN, C., KAMIO, T., FUJISAKA, H., HAEIWA, K. ISI and ICI compensation for TFI-OFDM in time-variant large delay spread channel. In *Proc. of ITC-CSCC2008*, pp. 1309-1312, July 2008.

About Authors...

Yuta IDA received the B.E. from Hiroshima City University, Japan, in 2008. Now, he is a master student in Hiroshima City University. His research interest is wireless communications.

Chang-Jun AHN received the Ph.D. degree at the Department of Information and Computer Science from Keio University, Japan in 2003. From 2001 to 2003, he was research associate in the Department of Information and Computer Science, Keio University. From 2003 to 2006, he was with the Communication Research Laboratory, Independent Administrative Institution (now the National Institute of Information and Communications Technology). In 2006, he was on assignment at ATR Wave Engineering Laboratories. Currently, he is working at the Faculty of Information Science, Hiroshima City University as an assistant professor. His current research interests include OFDM, digital communication, channel coding, and signal processing for telecommunications. He once served as an associate editor for Special Section on Multi-dimensional Mobile Information Network for the IEICE Trans. on Fundamentals. From 2005 to 2006, he was an expert committee member for emergence communication committee, Shikoku Bureau of Telecommunications, Ministry of Internal Affairs and Communications (MIC), Japan. Dr. Ahn received the ICF research grant award for Young Engineer in 2002 and the Funai Information Science Award for Young Scientist in 2003. He is member of IET (formerly IEE), IEICE, IEEE and the Korea Institute of Communication Science (KICS).

Takeshi KAMIO received the B.E., M.E. and Ph.D. degrees from Shizuoka University, Japan, in 1994, 1996 and 1999, respectively. From 1996 to 1999, he was a Research Fellow of the Japan Society for the Promotion of Science. In 1999, he joined the Faculty of Information Sciences, Hiroshima City University. Currently, he is a research associate in the Department of Systems Engineering. His research interests are design, learning methods, and applications of neural networks.

Hisato FUJISAKA received B.E., M.E., and Dr. Eng. degrees from Keio University, Japan in 1981, 1983, and 1994, respectively. He worked in the Department of Optical Communications, Osaki Electric Co. until 1997. He is currently an associate professor in the Faculty of Information Sciences, Hiroshima City University. His research interests include analysis and synthesis of nonlinear signal processing and communication circuits.

Kazuhisa HAEIWA graduated from the Department of Electrical Engineering, Tokushima University. He was engaged in the design and development of broadcasting transmitters. Since 2004, he has been a professor on the Faculty of Information Science, Hiroshima City University. He holds a D.Eng. Degree. In 1997, he received an Invention and Research Achievement Award from the Tokyo Metropolitan Award from the Tokyo Metropolitan Government. He also received a Development Award from the Image and Information Media Society in 1998 and an Advancement Award in 2001, IEICE member (fellow).